^{11}C-Labeled Analogs of Indomethacin Esters and Amides for Brain Cyclooxygenase-2 Imaging: Radiosynthesis, *in Vitro* Evaluation and *in Vivo* Characteristics in Mice

Yumi YAMAMOTO,[a] Jun TOYOHARA,[b] Kiichi ISHIWATA,[b] Kohei SANO,[a] Fumihiko YAMAMOTO,[a] Takahiro MUKAI,*[,a,c] and Minoru MAEDA*[,a]

[a] *Graduate School of Pharmaceutical Sciences, Kyushu University; 3–1–1 Maidashi, Higashi-ku, Fukuoka 812–8582, Japan:* [b] *Positron Medical Center, Tokyo Metropolitan Institute of Gerontology; 1–1 Naka-cho, Itabashi-ku, Tokyo 173–0022, Japan: and* [c] *Kobe Pharmaceutical University; 4–19–1 Motoyamakita-machi, Higashinada-ku, Kobe 658–8558, Japan.* Received January 5, 2011; accepted May 13, 2011; published online May 19, 2011

There is great potential in the use of positron emission tomography (PET) and suitable radiotracers for the study of cyclooxygenase type 2 (COX-2) enzyme in living subjects. In the present study, we prepared and evaluated five ^{11}C-labeled ester and amide analogs derived from indomethacin as potential PET imaging agents for the *in vivo* visualization of the brain COX-2 enzyme. Five ^{11}C-labeled COX-2 inhibitors, with different lipophilicities and moderate COX-2 inhibitory activity, were prepared by treatment of the corresponding *O*-desmethyl precursors with [^{11}C]methyl triflate and purified by HPLC (radiochemical yields of 55—71%, radiochemical purity of >93%, and the specific activities of 22—331 GBq/μmol). In mice, radioactivity in the brain for all radiotracers was low, with very low brain-to-blood ratios. A clear inverse relationship was observed between brain uptake at 1 min postinjection and the lipophilicity (experimental log $P_{7.4}$) of the studied ^{11}C-radiotracers. Pretreatment of mice with cyclosporine A to block P-glycoproteins caused a significant increase in brain uptake of radioactivity following injection of the ^{11}C-radiotracer compared to control. HPLC analysis showed that each radiotracer was rapidly metabolized, and a few metabolites, which were more polar than the original radiotracers, were found in both plasma and brain. No specific binding of the tracers towards the COX-2 enzyme in the brain was clearly revealed by *in vivo* blocking study. Further structural refinement of the tracer agent is necessary for better enhancement of brain uptake and for sufficient metabolic stability.

Key words cyclooxygenase type 2; indomethacin; carbon-11; brain; biodistribution; mouse

Cyclooxygenase (COX) is the crucial enzyme in the conversion of arachidonic acid to prostaglandins. It exists at least in two isoforms, a constitutive form (COX-1) and an inducible form (COX-2),[1—3] although a third distinct COX isozyme has also been reported.[4] The COX-1 enzyme is responsible for maintaining homeostasis whereas COX-2 is induced during inflammation by various stimuli and, in some tissues including the brain, kidney and placenta, is also constitutively expressed. Recent studies indicate that elevated expression of COX-2 has been implicated in many pathological events, including rheumatoid arthritis, cancer, heart disease, and neurodegenerative disorders.[5]

In the brain, COX-2 is mainly expressed in the cortex, hypothalamus, and hippocampus,[6] and is upregulated in neurological disorders such as Parkinson's disease and Alzheimer's disease,[7—9] although the functions of COX-2 in pathophysiological processes are not yet well-understood. There is great potential that COX-2-targeted imaging by positron emission tomography (PET) may provide useful information on the role of this enzyme, especially in various neurological disorders, and also may help to evaluate the efficacy of selective COX-2 inhibitors.[10] Thus, many COX-2 inhibitors have been labeled with a suitable radionuclide for mapping the enzymes *in vivo*. However, previously evaluated PET radiotracers, including ^{11}C-labeled COX inhibitors of the diarylheterocyclic class which were synthesized by us,[11,12] have only achieved limited success, due to a lack of sufficient specific-binding to the COX-2 enzyme and/or sufficient brain penetration, in spite of promising *in vitro* pharmacological data.[13—18] There is a need for systematic studies correlating the physicochemical properties of agents with their *in vivo* behavior for a better design of COX-2 imaging probes.

Currently, many selective COX-2 inhibitors with various structural features, as exemplified by vicinal diaryl heterocycles such as celecoxib and refecoxib, have been developed as non-steroidal anti-inflammatory drugs (NSAIDs) with improved gastric safety profiles.[19] Most of them have high lipophilicity. Indomethacin is a traditional non-selective inhibitor of the COX isozyme which is widely used as a NSAID, but with poor brain penetration largely due to the presence of the carboxylic acid moiety.[20] Interestingly, recent studies concerning ester and amide derivatives of indomethacin have found very high COX-2 inhibition potency and a high degree of COX-2-selectivity.[21—23] Marnett and colleagues synthesized ^{123}I-labeled *N*-iodobenzyl-containing amide derivative of indomethacin as a COX-2 imaging agent, which exhibited sufficient stability in COX-2 expressing nude mouse tumor.[24] More recently, using organic fluorophores tethered to indomethacin through an amide linkage, the feasibility of specific *in vivo* targeting of COX-2 in inflammatory lesions in mice has been demonstrated by the same group.[25]

The purpose of this study is to find suitable radioligands for imaging brain COX-2 *in vivo* by PET. We initially chose two potent and selective COX-2 inhibitors of indomethacin ester analog for ^{11}C-radiolabeling: *N*-Pentyl-(1-*p*-chlorobenzoyl-5-methoxy-2-methylindole)-3-acetate (**1**) (COX-1, IC_{50}>66 μM; COX-2, IC_{50}=50 nM)[21] and *N*-octyl-(1-*p*-chlorobenzoyl-5-methoxy-2-methylindole)-3-acetate (**2**) (COX-1, IC_{50}=66 μM; COX-2, IC_{50}=40 nM).[21] Furthermore, on the basis of the reported structure–activity studies concerning the ester and amide derivatives of indomethacin,[21—23] we

* To whom correspondence should be addressed. e-mail: m-maeda@daiichi-cps.ac.jp; mukai@phar.kyushu-u.ac.jp

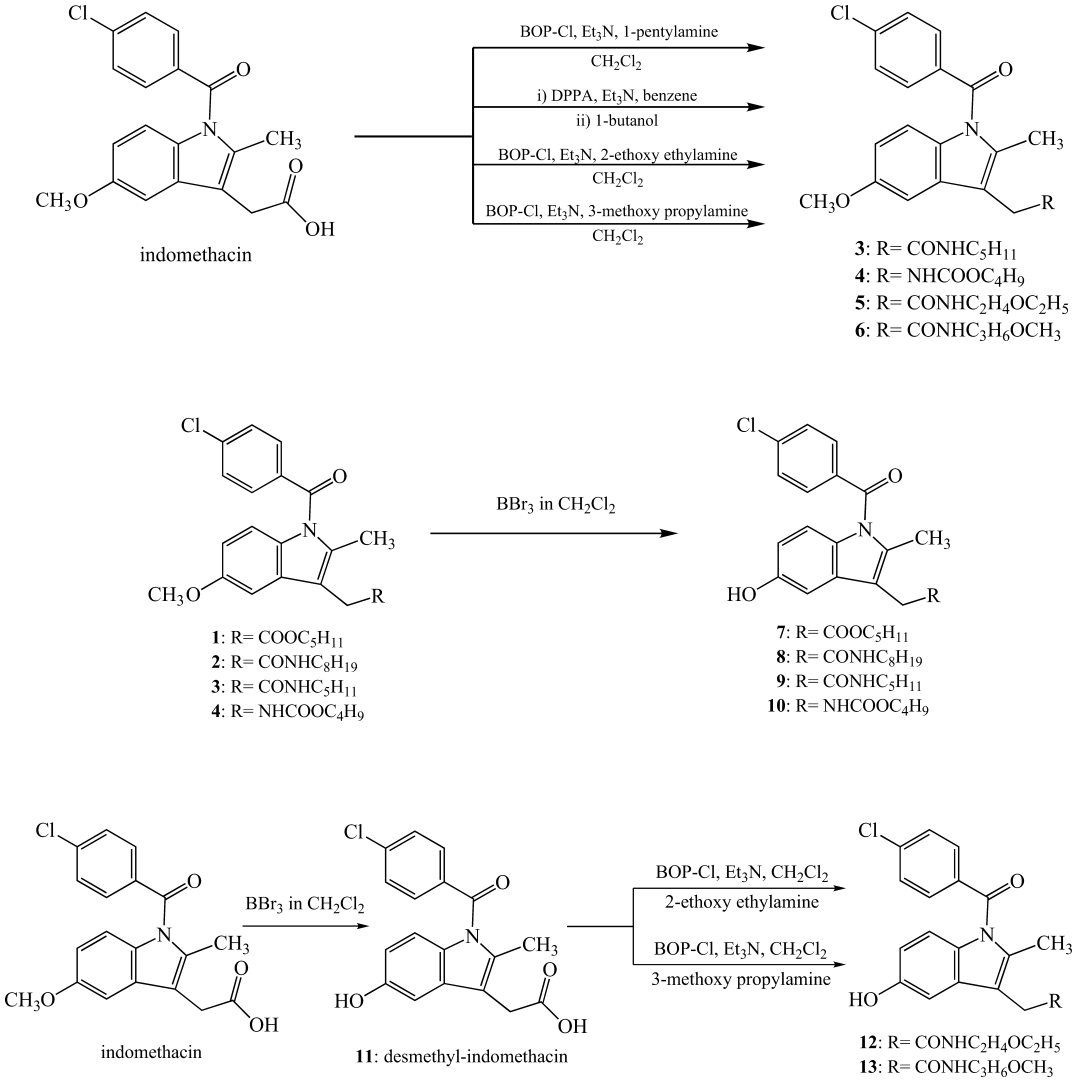

Chart 1. Synthesis Scheme for Indomethacin Esters and Amides (**3**—**6**), and Labeling Precursors (**7**—**10**, **12**, **13**)

next designed and synthesized one additional amide derivative, two amide compounds with a $–OCH_2–$ linkage, and one carbamate ester derivative of indomethacin, in order to examine the effects of different functional groups on COX-2 inhibitory potency and lipophilicity. As a consequence, five ^{11}C-labeled COX-inhibitors were prepared *via* demethyl precursors, and examined for *in vivo* characteristics in mice.

Results and Discussion

Synthesis Compounds **1** and **2** were prepared as previously described.[21] The target compounds (**3**, **5**, **6**) for HPLC standards and *in vitro* studies were obtained in satisfactory yields by treatment of indomethacin with the appropriate amine or alcohol according to a simlar literature procedure,[21] as illustrated in Chart 1. Additionally, the carbamate butyl ester (**4**) of indomethacin was obtained by Curtius rearrangement of the indomethacin azide, followed by treatment of intermediate isocyanate with 1-butanol. The phenolic precursors (**7**—**10**) for ^{11}C-radiolabeling were prepared in reasonable yields by demethylation of the corresponding indomethacin derivatives (**1**—**4**) using BBr_3 as a dealkylating agent. On the other hand, two phenolic compounds, **12** and **13**, with an alkoxy moiety in the side chain were obtained in a two-step procedure, in which demethylation of the methoxy group in indomethacin was achieved by treating it with BBr_3, and subsequent condensation of the carboxyl group with 2-ethoxyethylamine or 3-methoxypropylamine gave the desired compounds (Chart 1). All of the synthetic compounds gave satisfactory spectroscopic data, which were in full accordance with their depicted structures.

COX Inhibitory Activity The inhibitory activity of the compounds (**2**—**6**) for the COX enzyme and selectivity index (SI) was determined *in vitro*, including celecoxib and indomethacin as a reference COX inhibitor, using a colorimetric COX (ovine) inhibitor screening assay,[26] in which arachidonic acid was used as the substrate and *N*,*N*,*N*′,*N*′-tetramethylphenylenediamine (TMPD) as the cosubstrate. The IC_{50} value was calculated from the concentration–inhibition response curve. Additionally, the ratio of IC_{50} value of indomethacin as a reference compound-to-IC_{50} values of the test compounds was calculated to know the relative COX-2 inhibitory activity. *In vitro* inhibition studies showed that compound **3** had the highest affinity and selectivity for COX-2, followed by compound **2** (Table 1). These two compounds

have higher activity than celecoxib and indomethacin. The introduction of a $-OCH_2$ linkage instead of the methylene moiety in the side chain of indomethacin amide **3** significantly decreased the COX-2 inhibition potency with reduced selectivity (compounds **5**, **6**), which indicates that ether-oxygen may be detrimental to COX inhibition. Furthermore, compound **4** showed a significant loss of inhibition activity against both COX isoforms.

Radiolabeling Five ^{11}C-labeled indomethacin analogs [^{11}C]**1**—**3**, **5**, **6** were prepared by [^{11}C]-*O*-methylation of the corresponding demethyl precursors in acetone with [^{11}C]methyl triflate in the presence of NaOH as the base at room temperature, followed by purification with HPLC, as shown in Chart 2. Table 2 summarizes the results of the radiosyntheses. The presence of NaOH was essential for an efficient procedure for the desired methylation; however, for [^{11}C]-*O*-methylation of precursor **7**, the use of an excess amount of NaOH led to a more polar radioactive byproduct, consistent with the identity of ^{11}C-labeled indomethacin. Effective methylation of precursor **7** proceeded by the use of an equimolar amount of NaOH.[11] For [^{11}C]-*O*-methylations of the other four precursors, the use of a larger amount of NaOH successfully gave the required products. The absence of any residual of starting demethyl precursors in the purified product was verified by HPLC analysis.

Table 1. COX Inhibitory Activity of Six Indomethacin Esters and Amides, and Two Reference Compounds

Compound	IC_{50} (μM)[a]		Relative COX-2 inhibitory potency[b]	Selectivity[c]
	COX-1	COX-2		
1	—[d]	—[d]	—	—
2	>100	0.21	56	>476
3	>100	0.039	303	>2564
4	>100	>100	<0.1	—
5	>100	2.35	5	>42
6	>100	2.10	6	>47
Celecoxib	>100	0.56	21	>178
Indomethacin	0.79	11.8	1	0.067

a) Values represent the average of three independent determinations by colorimetric inhibition screening assay. *b*) Ratio of IC_{50} (indomethacin)/IC_{50} (test compound). *c*) Ratio of IC_{50} (COX-1)/IC_{50} (COX-2). *d*) IC_{50} of compound **1** could not be determined due to the lack of its chemical stability in the assay procedure.

Lipophilicity The partition coefficient of five ^{11}C-labeled compounds between 1-octanol and phosphate buffered saline was measured.[27] The log $P_{7.4}$ values were 1.98—3.94 (Table 2). Lipophilicity increased with increasing length of the side chain as seen in [^{11}C]**2** and [^{11}C]**3**, and replacement of the methylene of the side chain with oxygen as in [^{11}C]**5** and [^{11}C]**6** decreased log $P_{7.4}$ values due to its increased polarity. The measured values are somewhat in the outside range of those generally considered optimal for good blood brain barrier (BBB) penetration of drugs, although the well-known parabolic relationship between the lipophilicity of a molecule and its uptake by the brain is not universally applicable.[28,29] It should be noted that [^{11}C]**3** features a relatively low lipophilicity (log $P_{7.4}$=2.40) while retaining high COX-2 inhibitory potency and high selectivity, as shown in Table 1. In this study there was no correlation between the measured IC_{50} and log $P_{7.4}$ values for the compounds.

Biodistribution To explore the *in vivo* characteristics of the five ^{11}C-labeled compounds, biodistribution studies were performed in normal male ddY mice. The radioactivity concentrations in various tissues as a function of time following intravenous injection of the radiotracers are represented in Table 3. Four ^{11}C-radiotracers except for [^{11}C]**1** exhibited a relatively fast clearance of radioactivity in the blood within 60 min. The half-lives of the blood clearance were 12.3 min,

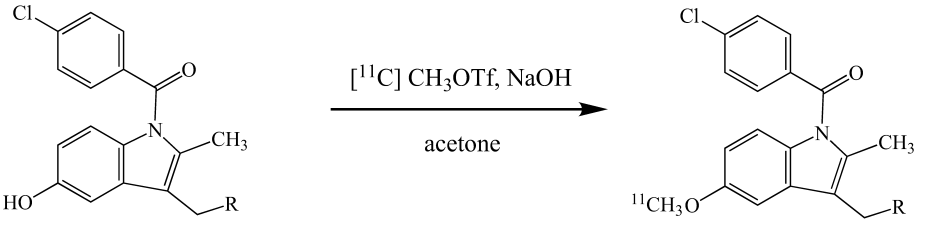

7: R= $COOC_5H_{11}$
8: R= $CONHC_8H_{19}$
9: R= $CONHC_5H_{11}$
12: R= $CONHC_2H_4OC_2H_5$
13: R= $CONHC_3H_6OCH_3$

[^{11}C] **1**: R= $COOC_5H_{11}$
[^{11}C] **2**: R= $CONHC_8H_{19}$
[^{11}C] **3**: R= $CONHC_5H_{11}$
[^{11}C] **5**: R= $CONHC_2H_4OC_2H_5$
[^{11}C] **6**: R= $CONHC_3H_6OCH_3$

Chart 2. Radiosynthesis of ^{11}C-Labeled Indomethacin Esters and Amides ([^{11}C]**1**, [^{11}C]**2**, [^{11}C]**3**, [^{11}C]**5**, [^{11}C]**6**)

Table 2. Summary of Radiosynthesis and Lipophilicity of ^{11}C-Labeled Indomethacin Esters and Amides

Compound	Radiochemical yield[a] %	Radiochemical purity %	Specific activity GBq/μmol	Log $P_{7.4}$[b]
[^{11}C]**1**	65±8 (n=4)	>97 (n=4)	22—61 (n=5)	3.94
[^{11}C]**2**	55±12 (n=5)	>94 (n=4)	29—97 (n=6)	3.78
[^{11}C]**3**	61±7 (n=3)	>93 (n=7)	38—135 (n=7)	2.40
[^{11}C]**5**	71±5 (n=4)	>96 (n=4)	166—295 (n=4)	2.12
[^{11}C]**6**	67±12 (n=4)	>96 (n=4)	149—331 (n=4)	1.98

a) Preparation time for 5 compounds was 21—27 min after the end of [^{11}C]CO_2 production. Decay-corrected yield based on [^{11}C]methyl triflate, average±S.D. (run numbers). *b*) The octanol/phosphate buffered saline (pH=7.4) partition coefficient (log $P_{7.4}$) using a conventional flask-shake technique, average of three independent assays.

Table 3a. Tissue Distribution of Radioactivity after Intravenous Injection of [^{11}C]**1** into Mice

Tissue	Uptake (%ID/g)[a]			
	1 min	5 min	30 min	60 min
Blood	10.73±0.94	8.80±1.02	6.36±0.37	4.95±0.29
Brain	0.47±0.09	0.45±0.06	0.34±0.06	0.23±0.02
Heart	6.81±1.18	5.11±0.75	2.69±0.37	2.17±0.23
Lung	10.06±1.54	4.38±0.15	3.63±0.39	3.49±0.11
Liver	12.43±1.75	6.54±1.38	6.22±0.43	5.53±0.33
Kidney	7.57±0.74	8.25±0.83	7.88±0.46	6.94±1.13
Small intestine	2.20±0.36	3.56±0.80	3.73±0.74	3.15±0.47

a) Mean±S.D. (n=4).

Table 3b. Tissue Distribution of Radioactivity after Intravenous Injection of [^{11}C]**2** into Mice

Tissue	Uptake (%ID/g)[a]			
	1 min	5 min	30 min	60 min
Blood	3.75±0.50	1.15±0.11	0.83±0.11	0.79±0.13
Brain	0.18±0.08	0.19±0.06	0.26±0.07	0.25±0.05
Heart	5.65±0.57	3.95±0.75	0.74±0.05	0.59±0.08
Lung	14.48±3.00	6.60±0.75	1.86±0.96	1.43±0.73
Liver	16.11±0.62	14.58±2.44	8.07±0.88	5.59±0.22
Kidney	5.79±0.40	5.13±0.66	2.16±0.42	1.84±0.25
Small intestine	1.71±0.30	12.01±0.68	6.90±0.85	5.36±2.07

a) Mean±S.D. (n=4).

Table 3c. Tissue Distribution of Radioactivity after Intravenous Injection of [^{11}C]**3** into Mice

Tissue	Uptake (%ID/g)[a]			
	1 min	5 min	30 min	60 min
Blood	3.50±0.18	1.80±0.23	0.73±0.06	0.72±0.13
Brain	1.06±0.09	0.98±0.09	0.51±0.09	0.48±0.13
Heart	7.05±0.36	2.36±0.18	0.80±0.15	0.59±0.11
Lung	6.26±0.53	4.18±1.82	2.79±2.44	0.76±0.13
Liver	12.98±1.52	10.03±1.70	5.40±0.85	4.87±0.98
Kidney	10.95±1.19	5.40±0.43	1.84±0.30	1.42±0.27
Small intestine	3.49±0.41	6.15±1.39	2.50±0.56	3.16±0.85

a) Mean±S.D. (n=4).

Table 3d. Tissue Distribution of Radioactivity after Intravenous Injection of [^{11}C]**5** into Mice

Tissue	Uptake (%ID/g)[a]			
	1 min	5 min	30 min	60 min
Blood	2.13±0.09	1.50±0.10	0.80±0.12	0.86±0.22
Brain	1.53±0.09	1.10±0.05	0.52±0.04	0.52±0.25
Heart	4.61±0.25	2.30±0.10	0.77±0.09	0.61±0.10
Lung	3.73±0.69	2.29±0.21	0.93±0.14	0.76±0.17
Liver	7.65±1.23	10.70±1.27	5.25±0.73	4.64±1.69
Kidney	7.76±0.54	3.54±0.19	1.61±0.16	1.26±0.24
Small intestine	4.03±0.44	10.71±2.71	4.12±1.35	3.20±1.79

a) Mean±S.D. (n=4).

1.3 min, 2.9 min, 4.2 min, and 3.8 min for [^{11}C]**1**, [^{11}C]**2**, [^{11}C]**3**, [^{11}C]**5**, and [^{11}C]**6**, respectively. The highest initial concentrations of radioactivity were observed in the liver for all tracers, followed by a gradual increase and/or relatively slow clearance of radioactivity. In addition, the peak concentration of radioactivity observed in the small intestine may reflect hepatobiliary clearance of the parent tracers and/or their radioactive metabolites. [^{11}C]**1** displayed very high levels of radioactivity in the blood and most organs such as the liver, lungs and kidneys in contrast to the other four radiotracers.

Table 3e. Tissue Distribution of Radioactivity after Intravenous Injection of [^{11}C]**6** into Mice

Tissue	Uptake (%ID/g)[a]			
	1 min	5 min	30 min	60 min
Blood	3.01±0.28	1.92±0.20	1.05±0.13	0.84±0.08
Brain	1.84±0.16	1.12±0.11	0.65±0.17	0.41±0.07
Heart	6.09±0.25	2.73±0.23	0.92±0.08	0.57±0.04
Lung	5.38±0.40	2.91±0.29	1.07±0.14	0.73±0.02
Liver	11.68±2.35	14.90±2.45	13.95±1.24	9.15±0.69
Kidney	10.28±1.39	4.67±0.62	2.59±0.27	1.82±0.06
Small intestine	5.12±1.10	8.39±2.47	8.32±1.78	7.26±2.14

a) Mean±S.D. (n=4).

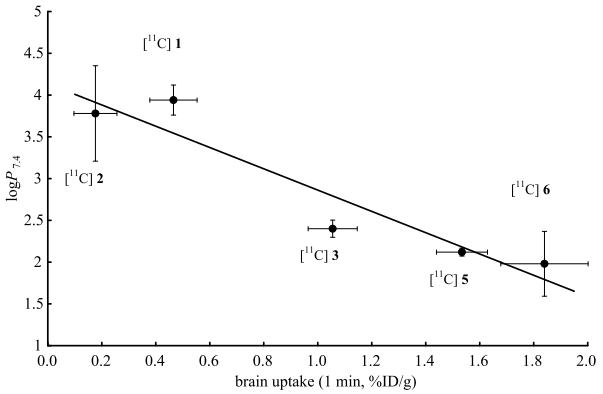

Fig. 1. Relationship between Lipophilicity ($\log P_{7.4}$) and Mouse Brain Uptake (%ID/g) at 1 min after Injection of the ^{11}C-COX Inhibitors

Whole brain uptake for all tracers was low, with values ranging from 0.18% injected dose (ID)/g for [^{11}C]**2** to 1.84% ID/g for [^{11}C]**6** at 1 min after administration which, with exception of [^{11}C]**2**, then decreased slowly over 60 min. In the case of [^{11}C]**2** which showed the lowest brain uptake, a slight increase of radioactivity in the brain was observed at later time points. The brain-to-blood ratios of all tracers were consequently much less than 1.0 unity (0.04—0.77) throughout the observation period. These results clearly demonstrate that all tracers investigated have low BBB permeability. Notably, the lipophilicity of the radiotracers inversely correlated well (r^2=0.90, p=0.01) with brain uptake at 1 min post injection (Fig. 1), which is most likely to be reflective of the initial extraction of the radiotracers from the blood. This relationship may be due to binding to plasma proteins which is expected to increase with larger $\log P_{7.4}$ values of the indomethacin analogs.[30] These radiotracers likely bind to the plasma proteins similar to other NSAIDs, including indomethacin binding with high affinity to serum albumin.[31,32] Non-specific binding to albumin and other plasma proteins is known to correlate positively and linearly *in vitro* with increasing lipophilicity. However, it remains controversial the extent to which non-specific binding to plasma proteins inhibits BBB penetration. This theory cannot explain why some radiotrac-

ers exhibiting high (>90%) plasma protein binding may enter the brain nearly as well as those that exhibit much lower plasma protein binding.[29] Certainly, some tracers including [^{11}C]palmitic acid[33] and [^{11}C]arachidonic acid[34,35] with calculated log P>7 have been used successfully in PET experiments although their maximal brain uptakes are lower than those of commonly used neuroreceptor radioligands. Therefore, lipophilicity is, in any case, an imperfect proxy for BBB permeability. Currently, there is no general understanding of the relationship between lipophilicity and the distribution characteristics for radiotracers of COX-2 inhibitors. Unfortunately, high lipophilicity is inherent in currently available COX inhibitors because of hydrophobic interactions with the COX binding sites in both isozymes.[36]

Metabolism in Plasma and Brain The metabolic behavior of each radiotracer *in vivo* was studied in mice at 30 min after injection. As summarized in Table 4, each radiotracer was rapidly metabolized. HPLC analysis of plasma for [^{11}C]**1** showed no unchanged form and one polar peak (polar 1) of which the retention time corresponds to that of indomethacin. In the other four tracers, 14—32% of the radioactivity was recovered as unchanged parent compounds, and a few radiolabeled metabolites including [^{11}C]indomethacin (polar 1) were found. The findings seemingly indicated hydrolysis of the ester or amide moiety of the tracers by esterase in the blood and peripheral organs. Unidentified more polar metabolites (polar 3) were predominant for both [^{11}C]**3** and [^{11}C]**5**. Remmel *et al.* have shown for indomethacin phenethylamide in rodents that the initial step in the metabolism is the oxidative pathway on its amide side chain, resulting in the formation of hydroxylated and *O*-demethylated metabolites in addition to their glucuronides.[37] If this route of metabolism is also the case for the radiotracers studied here, then more polar metabolites than the parent compounds would be produced.

Table 4. ^{11}C-Labeled Metabolites in Plasma and Brain at 30 min after Intravenous Injection of ^{11}C-Labeled Indomethacin Esters and Amides into Mice

		Percentage of metabolite[a]			
		Parent	Polar 1 (indomethacin)	Polar 2	Polar 3
[^{11}C]**1**	Retention time[b]	8.0 min	2.9 min	2.1 min	
	Plasma	ND	100	ND	
	Brain	26±6	52±3	22±9	
[^{11}C]**2**	Retention time[b]	13.2 min	5.2 min	4.1 min	
	Plasma	15±4	72±3	13±1	
	Brain	22±4	ND[c]	ND[c]	
[^{11}C]**3**	Retention time[b]	6.7 min	4.8 min	3.3 min	2.1 min
	Plasma	32±5	11±2	14±5	43±7
	Brain	21±7	6±4	ND	73±7
[^{11}C]**5**	Retention time[b]	12.7 min	8.1 min	5.3 min	3.9 min
	Plasma	17±4	28±8	9±5	46±9
	Brain	9±2	7±4	ND	84±5
[^{11}C]**6**	Retention time[b]	11.0 min	8.4 min	6.6 min	4.2 min
	Plasma	14±5	41±6	20±8	25±17
	Brain	9±2	7±1	ND	84±3

a) Mean±S.D. (n=3), ND=not detected. *b*) Retention time on HPLC analysis. *c*) Besides a parent peak, 78% of the radioactivity was eluted with the broadening of peaks including polar 1 and polar 2 and metabolite profiles could not be accurately determined.

In the brain samples only 9—26% of the radioactivity was detected as intact forms and the presence of two radiolabeled metabolites, [^{11}C]indomethacin (polar 1) and an unidentified fraction (polar 2), was found. A polar 3 metabolite observed in plasma extracts was absent in the brain samples. The metabolism probably occurred in the brain because plasma metabolites are expected to poorly penetrate the BBB. However, this consideration requires further investigation. Thus, one of the reasons for the low accumulation of radioactivity in the brain has been found in the marked metabolism of the studied ^{11}C-labeled radiotracers, which occurred in the plasma and brain tissue. However, a low initial uptake of each radiotracer was not explained by the rapid metabolism.

Specific Binding To determine the specific binding of radiotracers to COX-2 enzymes, blocking experiments were carried out using several COX-2 selective inhibitors with BBB permeability, celecoxib and *N*-[2-(cyclohexyloxy)-4-nitrophenyl]methanesulfonamide (NS-398), a nonselective COX inhibitor, indomethacin, and carrier-loading. None of any COX inhibitors and each unlabeled compound caused significant inhibition in the brain uptake and brain-to-blood ratio of [^{11}C]**1**, [^{11}C]**2**, [^{11}C]**5** or [^{11}C]**6** as summarized in Table 5 which involves the representative blocking results with celecoxib and NS-398, suggesting the absence of COX-2-specific and saturable binding. On the other hand, in the case of [^{11}C]**3**, a small but statistically significant inhibition (*ca.* 15% reduction) was observed in the brain uptake of radioactivity with celecoxib or NS-398 (Table 5). This finding seems to indicate a small fraction of displaceable binding in the brain, but additional evidence is necessary. The rapid degradation of all ^{11}C-COX inhibitors and the presence of radiometabolites in the brain as described above can also contribute to the lack of specific binding for COX-2 enzyme *in vivo* blocking.

Effect of Cyclosporine A The BBB expresses various

Table 5. Radioactivity of ^{11}C-COX Inhibitors in the Brain and the Blood of Mice Co-injected with COX-2 Inhibitor, Celecoxib and NS-398[a]

	Brain uptake (%ID/g)[b]			Brain-to-blood ratio[b]		
	Control	Celecoxib	NS-398	Control	Celecoxib	NS-398
[^{11}C]**1**	0.54±0.13	0.46±0.07	0.42±0.07	0.08±0.01	0.08±0.01	0.07±0.01
[^{11}C]**2**	0.40±0.04	0.34±0.09	0.48±0.13	0.46±0.02	0.41±0.08	0.52±0.11
[^{11}C]**3**	0.68±0.08	0.58±0.09*	0.71±0.09	0.86±0.20	0.67±0.06*	0.67±0.06*
[^{11}C]**5**	0.73±0.12	0.72±0.09	0.79±0.08	0.66±0.08	0.60±0.18	0.88±0.27
[^{11}C]**6**	0.80±0.06	0.76±0.04	0.73±0.09	0.62±0.03	0.60±0.03	0.51±0.12

a) Mice received the following blocker solution (1 mg/kg per animal, 0.1 ml), celecoxib, and NS-398 dissolved in DMSO, co-injected with each radiotracer. In the control mice the same amount of DMSO was co-injected. The radioactivity in the tissue was measured at 30 min for [^{11}C]**2** and [^{11}C]**3**, and at 15 min for [^{11}C]**5** and [^{11}C]**6** after each ^{11}C-COX inhibitor injection. *b*) Mean±S.D. (n=5). * Significant decrease (p<0.05) compared to the control (Student's t-test).

Table 6. Effect of P-Glycoprotein Modulation with Cyclosporine A on the Brain Uptake of Radioactivity after Intravenous Injection of ^{11}C-COX Inhibitors into Mice[a)]

	Brain uptake (%ID/g)[b)]			Brain-to-blood ratio[b)]		
	Control	CysA	CysA/Control	Control	CysA	CysA/Control
[^{11}C]**2**	0.40±0.04	1.55±1.04*	3.88	0.46±0.02	1.27±0.85*	2.76
[^{11}C]**3**	0.68±0.08	0.99±0.09**	1.46	0.86±0.20	0.90±0.05	1.05
[^{11}C]**5**	0.73±0.12	1.11	1.52	0.66±0.08	0.92	1.39
[^{11}C]**6**	0.80±0.06	1.71±0.25**	2.13	0.62±0.03	1.20±0.25**	1.94

a) Mice were pretreated with cyclosporine A (CysA) (50 mg/kg, i.v.) 30 min before injection of the tracers, and the radioactivity in the tissue was measured at 30 min for [^{11}C]**2** and [^{11}C]**3**, and at 15 min for [^{11}C]**5** and [^{11}C]**6** after each ^{11}C-COX inhibitor injection. *b*) Mean±S.D. (CysA; $n=4$ for [^{11}C]**2** and [^{11}C]**6**, $n=5$ for [^{11}C]**3**, $n=2$ for [^{11}C]**5.** control; $n=5$ for each group). * $p<0.05$ and ** $p<0.01$, compared to the control (Student's *t*-test).

transporters such as P-glycoprotein (P-gp) (also called as ABCB1) and multidrug resistance-associated proteins (MRPs).[38] Recently, the modulation of several PET-radioligands by P-gp *in vivo* has been evaluated in rodents, showing that P-gp plays an important role in restricting brain uptake of radioligands.[39,40] Low brain uptakes of four radiotracers may attribute to the P-gp. Zrieki *et al.* reported that the heptyl ester derivative of indomethacin is neither a substrate nor a competitive inhibitor of P-gp in Caco-2 cells.[41] On the other hand, in a previous study, we found that 2-(4-aminosulfonylphenyl)-3-(8-methoxyphenyl)-indole with high COX-2-inhibiting activity was found to be a substrate for the P-gp in *in vitro* monolayer efflux assays, but its ^{11}C-labeled analog was not sensitive to P-gp modulation with cyclosporine (Cys) A *in vivo*.[12] In this study, we investigated P-gp modulation of four radiotracers, although they were not applied to the *in vitro* monolayer efflux assays. As shown in Table 6, pretreatment with CysA (50 mg/kg) seemed to slightly enhanced brain uptake and/or the brain-to-blood ratio for [^{11}C]**2**, [^{11}C]**3**, [^{11}C]**5** and [^{11}C]**6** with and without statistical significance, thus seemingly indicating a possible contribution of P-gp-mediated transport of these ^{11}C-tracers. CysA has several peripheral effects, not mediated by P-gp blockade, such as inhibition of cytochrome P450 and toxicity to liver and kidney.[42,43] In this study we found that each radiotracer suffered extensive metabolism and that two or three radiometabolites were present in both brain and plasma tissues with high levels of radioactivity, although the metabolic profile was measured at a one-time point (15 or 30 min postinjection). Considering these findings, this modest increase in cerebral uptake of radioactivity induced by CysA, was probably caused by altered cytochrome P450-mediated metabolism, rather than a P-gp-mediated efflux of the parent radiotracer itself.[37,44]

Conclusion

This paper describes the effect of altering the structure of the alkyl side chain of indomethacin esters and amides in regard to COX-2 inhibitory potency and *in vivo* brain uptake in order to find a suitable radiotracer candidate for imaging brain COX-2. The *in vivo* behavior of all radiotracers in mice is characterized by low brain uptake and fast metabolic susceptibility. No specific binding of the radiotracers toward the COX-2 enzyme in the brain was clearly revealed, although [^{11}C]**3** seemed to show a small specific signal. It should be noted that there was an inverse correlation between the brain uptake of radioactivity at 1 min postinjection and the lipophilicity values ($\log P_{7.4}$) of the ^{11}C-tracers investigated here, although the small number of radiotracers ($n=5$), suggesting that the lipophilicity could be used to predict the BBB permeability for derivatives of indomethacin and related compounds. In this study, we found that one compound [^{11}C]**3** features relatively low lipophilicity ($\log P_{7.4}=2.40$) while retaining high COX-2 inhibitory potency and high selectivity. This might be good news for guiding the design of COX-2 selective radiotracers. Further structural refinement of the radiotracers is necessary to achieve better enhancement of brain uptake and sufficient metabolic stability.

Experimental

General *N*-Pentyl-(1-*p*-chlorobenzoyl-5-methoxy-2-methylindole)-3-acetate (**1**), *N*-octyl-(1-*p*-chlorobenzoyl-5-methoxy-2-methylindole)-3-acetamide (**2**)[21] and celecoxib[45] were prepared as previously described. Other chemical reagents and solvents were of special grade and were used without further purification unless otherwise noted.

^{1}H-NMR spectra were recorded on a Varian Unity 400 (400 MHz, California, U.S.A.) and the chemical shifts are referenced to trimethylsilane (TMS) ($\delta=0$ ppm). IR spectra were recorded with a Shimadzu FTIR-8400 spectrometer (Kyoto, Japan) and mass spectra were obtained with a JEOL JMS DX-610 (FAB Mass, Tokyo, Japan) or an Applied Biosystems Mariner System 5299 spectrometer (electrospray ionization (ESI) MS, California, U.S.A.). All melting points were determined on a Yanaco melting point apparatus (Yanagimoto Ind. Co., Kyoto, Japan) and are uncorrected. Column chromatography was performed on Silica gel 60N (63—210 mesh, Kanto Chemical Co., Tokyo, Japan). The progress of the reaction was monitored by TLC on Silica gel 60F 254 plates (Merck, Darmstadt, Germany) and spots were visualized with UV light or iodine. In the synthetic procedures, the organic extracts were routinely dried over anhydrous Na_2SO_4 and evaporated with a rotary evaporator.

Preparation of [^{11}C]methyl triflate from [^{11}C]CO_2 *via* [^{11}C]methyl iodide and subsequent ^{11}C-methylation were carried out automatically by using a synthetic apparatus for ^{11}C-labeled compounds at the Tokyo Metropolitan Institute of Gerontology. Preparative HPLC was done using a Shimadzu Liquid Chromatograph System (SPD-10A, Kyoto, Japan), equipped with a UV detector set at 260 nm and a semiconductor radiation detector system under the indicated conditions. Radiochemical purity and specific radioactivity of the labeled compounds were determined by the same HPLC system under the indicated conditions. The radioactivity was also quantified with an auto-well gamma counter (LKB Wallac Compugamma 1282CS, Turku, Finland). HPLC for metabolite analysis was done with a Shimadzu Liquid Chromatograph System (SPD-6AVA, Kyoto, Japan) having a UV detector set at 260 nm, and a packed flow scintillation analyzer 150TR (PerkinElmer, Waltham, MA, U.S.A.).

Male ddY mice (7—8 weeks old) were obtained from Tokyo Laboratory Animals (Tokyo, Japan). The animal studies were approved by the Animal Care and Use Committee of the Tokyo Metropolitan Institute of Gerontology.

***N*-Pentyl-(1-*p*-chlorobenzoyl-5-methoxy-2-methylindole)-3-acetamide (3)** According to the procedure reported by Marnett and colleagues,[21] a reaction mixture containing indomethacin (1000 mg, 2.8 mmol) and bis-(2-oxo-3-oxazolidinyl)phosphinic chloride (727 mg, 2.8 mmol, 1 eq) in anhydrous CH_2Cl_2 (20 ml) was treated with Et_3N (770 μl, 5.5 mmol, 2 eq) and allowed to stir at room temperature for 10 min. The mixture was then treated with 1-pentylamine (371 μl, 3.2 mmol, 1.1 eq) and stirred overnight at room temperature. The reaction mixture was filtered and the filtrate was concen-

trated *in vacuo*. The residue was purified by chromatography on silica gel with hexane : EtOAc = 3 : 1 to provide **3** (843 mg, 70.6%) as a pale yellow solid: mp 137—138 °C; ^{1}H-NMR ($CDCl_3$) δ: 7.66 (2H, d, J=8.4 Hz), 7.49 (2H, d, J=8.4 Hz), 6.87 (2H, m), 6.70 (1H, dd, J=2.4, 9.2 Hz), 5.56 (1H, s), 3.82 (3H, s), 3.63 (2H, s), 3.20 (2H, m), 2.38 (3H, s), 1.39 (2H, m), 1.21 (4H, m), 0.83 (3H, t, J=7.2 Hz); Fourier transform (FT)-IR (KBr) cm^{-1}: 3300, 1670, 1638; FAB-MS m/z: 427.25 $(M+H)^+$. HR-MS: Calcd for $C_{24}H_{28}ClN_2O_3$ $(M+H)^+$: 427.1783, 429.1764. Found 427.1795, 429.1804.

Butyl-(1-*p*-chlorobenzoyl-5-methoxy-2-methylindole)-3-yl Methylcarbamate (4) A solution of indomethacin (500 mg, 1.4 mmol) and diphenylphosphoryl azide (1.2 ml, 5.6 mmol, 4 eq) in dry benzene (22 ml) in the presence of Et_3N (3.8 ml, 27.5 mmol, 20 eq) was heated under reflux for 1 h. After adding 1-butanol (25 ml, 272.5 mmol, 194 eq), the reaction solution was further heated for 1.5 h, cooled, and concentrated *in vacuo*. The residue was dissolved in EtOAc, filtered through a short path of celite, and the solvent was removed *in vacuo*. The residue was purified by chromatography on silica gel with $CHCl_3$: hexane : acetone = 5 : 90 : 5 to provide **4** (414 mg, 69.1%) as a pale yellow solid: mp 103—107 °C; ^{1}H-NMR ($CDCl_3$) δ: 7.65 (2H, d, J=8.4 Hz), 7.47 (2H, d, J=8.0 Hz), 7.03 (1H, m), 6.83 (1H, d, J=8.8 Hz), 6.67 (1H, dd, J=2.4, 8.8 Hz), 4.74 (1H, s), 4.47 (2H, d, J=5.6 Hz), 4.10 (2H, m), 3.83 (3H, s), 2.42 (3H, s), 1.59 (2H, m), 1.38 (2H, m), 0.92 (3H, t, J=7.2 Hz); FT-IR (KBr) cm^{-1}: 3379, 1721; FAB-MS m/z: 428.2 $(M)^+$. HR-MS: Calcd for $C_{23}H_{26}ClN_2O_4$ $(M+H)^+$: 429.1576. Found 429.1613.

***N*-2-Ethoxyethyl-(1-*p*-chlorobenzoyl-5-methoxy-2-methylindole)-3-acetamide (5)** Compound **5** was obtained in a similar manner to the synthesis of **3** from indomethacin using 2-ethoxy ethylamine. The crude product was purified by chromatography on silica gel with hexane : EtOAc = 2 : 1 to provide **5** (580 mg, 48.4%) as a pale yellow solid: mp 99—102 °C; ^{1}H-NMR ($CDCl_3$) δ: 7.72 (2H, d, J=8.4 Hz), 7.48 (2H, d, J=8.8 Hz), 6.90 (1H, d, J=2.4 Hz), 6.86 (1H, d, J=9.2 Hz), 6.69 (1H, dd, J=2.6 Hz, 9.0 Hz), 6.00 (1H, s), 3.82 (3H, s), 3.64 (2H, s), 3.40 (4H, s), 3.34 (2H, m), 2.39 (3H, s), 1.00 (3H, t, J=7.0 Hz); FT-IR (KBr) cm^{-1}: 3325, 2924, 1681, 1637; FAB-MS m/z: 429.3 $(M+H)^+$. HR-MS: Calcd for $C_{23}H_{26}ClN_2O_4$ $(M+H)^+$: 429.1576, 431.1557. Found 429.1560, 431.1587.

***N*-3-Methoxypropyl-(1-*p*-chlorobenzoyl-5-methoxy-2-methylindole)-3-acetamide (6)** Compound **6** was obtained in a similar manner to the synthesis of **3** from indomethacin using 3-methoxy propylamine. The crude product was purified by chromatography on silica gel with hexane : EtOAc = 3 : 2 to provide **6** (600 mg, 50%) as a pale yellow solid: mp 119—121 °C; ^{1}H-NMR ($CDCl_3$) δ: 7.67 (2H, d, J=8.6 Hz), 7.48 (2H, d, J=8.5 Hz), 6.88 (2H, m), 6.70 (1H, dd, J=2.4, 8.9 Hz), 6.23 (1H, s), 3.83 (3H, s), 3.61 (2H, s), 3.33 (4H, m), 3.01 (3H, s), 2.36 (3H, s), 1.66 (2H, q, J=6.0 Hz); FT-IR (KBr) cm^{-1}: 3269, 2922, 1695, 1643; FAB-MS m/z: 429.1 $(M+H)^+$. HR-MS: Calcd for $C_{23}H_{26}ClN_2O_4$ $(M+H)^+$: 429.1576, 431.1557. Found 429.1600, 431.1591.

***N*-Pentyl-(1-*p*-chlorobenzoyl-5-hydroxy-2-methylindole)-3-acetate (7)** Boron tribromide (BBr_3) (1 M in CH_2Cl_2, 0.8 ml, 0.8 mmol, 6.8 eq) was added dropwise to an ice-cooled solution of **1** (50 mg, 117 μmol) in anhydrous CH_2Cl_2 (3 ml). The reaction mixture was stirred at 5 °C for 0.5 h. After stirring overnight at room temperature, the reaction mixture was diluted with water and extracted with CH_2Cl_2. The combined organic phase was washed with water, dried and filtered, and the solvent was removed *in vacuo*. The residue was purified by chromatography on silica gel with $CHCl_3$: methanol = 99 : 1 to provide **7** (44 mg, 90.2%) as a dark brown solid: mp 72—74 °C: ^{1}H-NMR ($CDCl_3$) δ: 7.65 (2H, d, J=8.4 Hz), 7.47 (2H, d, J=8.0 Hz), 6.92 (1H, s), 6.86 (1H, d, J=8.6 Hz), 6.58 (1H, d, J=9.2 Hz), 4.60 (1H, s), 4.09 (2H, m), 3.62 (2H, s), 2.36 (3H, s), 1.61 (2H, m), 1.29 (4H, m), 0.86 (3H, t, J=6.6 Hz); FT-IR (neat) cm^{-1}: 3400, 2929, 1681; FAB-MS m/z: 413.2 $(M)^+$. HR-MS: Calcd for $C_{23}H_{25}ClNO_4$ $(M+H)^+$: 414.1467, 416.1448. Found 414.1448, 416.1428.

***N*-Octyl-(1-*p*-chlorobenzoyl-5-hydroxy-2-methylindole)-3-acetamide (8)** Compound **8** was obtained in a similar manner as **7** by demethylation of **2** using BBr_3. The crude product was purified by chromatography on silica gel with $CHCl_3$: acetone = 17 : 1 to give **8** (134 mg, 92.0%) as a pale yellow solid: mp 192—194 °C; ^{1}H-NMR (DMSO-d_6) δ: 9.09 (1H, s), 7.87 (1H, m), 7.68 (2H, d, J=8.8 Hz), 7.63 (2H, d, J=8.4 Hz), 6.89 (2H, m), 6.55 (1H, d, J=8.8 Hz), 3.41 (2H, s), 3.03 (2H, m), 2.18 (3H, s), 1.39 (2H, m), 1.22 (10H, m), 0.84 (3H, t, J=6.6 Hz); FT-IR (KBr) cm^{-1}: 3332, 3219, 2925, 2856; FAB-MS m/z: 455.3 $(M+H)^+$. HR-MS: Calcd for $C_{26}H_{32}ClN_2O_3$ $(M+H)^+$: 455.2096. Found 455.2131.

***N*-Pentyl-(1-*p*-chlorobenzoyl-5-hydroxy-2-methylindole)-3-acetamide (9)** Compound **9** was obtained in a similar manner as **7** by demethylation of **3** using BBr_3. The crude product was purified by chromatography on silica gel with hexane : EtOAc = 3 : 1 to give **9** (55 mg, 57.3%) as a dark brown solid: mp 194—195 °C; ^{1}H-NMR ($CDCl_3$) δ: 7.67(2H, d, J=8.8 Hz), 7.48 (2H, d, J=8.4 Hz), 6.85 (2H, m), 6.64 (1H, dd, J=2.4, 8.8 Hz), 6.18 (1H, s), 5.61 (1H, s), 3.62 (3H, s), 3.20 (2H, m), 2.37 (3H, s), 1.40 (2H, m), 1.26 (4H, m), 0.82 (3H, t, J=7.2 Hz); FT-IR (KBr) cm^{-1}: 3212, 1665, 1641; FAB-MS m/z: 413.2 $(M+H)^+$. HR-MS: Calcd for $C_{23}H_{26}ClN_2O_3$ $(M+H)^+$: 413.1626, 415.1607. Found 413.1672, 415.1653.

Butyl-(1-*p*-chlorobenzoyl-5-hydroxy-2-methylindole)-3-ylmethylcarbamate (10) Compound **10** was obtained in a similar manner as **7** by demethylation of **4** using BBr_3. The crude product was purified by chromatography on silica gel with hexane : EtOAc = 4 : 1 to give **10** (106 mg, 73.3%) as a beige powder: mp 91—93 °C; ^{1}H-NMR ($CDCl_3$) δ: 7.65 (2H, d, J=8.4 Hz), 7.47 (2H, d, J=8.4 Hz), 7.00 (1H, s), 6.81 (1H, d, J=8.8 Hz), 6.60 (1H, dd, J=2.4, 8.8 Hz), 5.19 (1H, s), 4.77 (1H, s), 4.44 (2H, d, J=5.2 Hz), 4.12 (2H, m), 2.40 (3H, s), 1.38 (2H, m), 1.26 (2H, m), 0.92 (3H, m); FT-IR (neat) cm^{-1}: 3327, 1686; FAB-MS m/z: 415.26 $(M+H)^+$.

1-*p*-Chlorobenzoyl-5-hydroxy-2-methylindole-3-acetatic Acid (11) Compound **11** was obtained in a similar manner as **7** by demethylation of indomethacin using BBr_3. The crude product was purified by chromatography on silica gel with CH_3Cl : acetone = 2 : 1 to give **11** (543 mg, 56.5%) as a white powder: mp 223—225 °C; ^{1}H-NMR (DMSO-d_6) δ: 9.16 (1H, s), 7.65 (4H, q, J=6.0, 8.8 Hz), 6.86 (1H, d, J=8.8 Hz), 6.82 (1H, d, J=2.0 Hz), 6.55 (1H, dd, J=2.4, 8.8 Hz), 3.57 (2H, s), 2.19 (3H, s); FAB-MS m/z: 344.2 $(M+H)^+$. HR-MS: Calcd for $C_{18}H_{14}ClNO_4$ $(M+H)^+$: 344.0684. Found 344.0712.

***N*-2-Ethoxyethyl-(1-*p*-chlorobenzoyl-5-hydroxy-2-methylindole)-3-acetamide (12)** Compound **12** was obtained in a similar manner to the synthesis of **3** from **11** using 2-ethoxy ethylamine. The crude product was purified by chromatography on silica gel with $CHCl_3$: acetone = 9 : 1 to give **12** (74 mg, 33.7%) as a pale yellow solid: mp 112—114 °C; ^{1}H-NMR ($CDCl_3$) δ: 7.66 (2H, d, J=8.8 Hz), 7.30 (2H, d, J=8.4 Hz), 6.86 (1H, d, J=2.0 Hz), 6.80 (1H, d, J=8.8 Hz), 6.66 (1H, s), 6.62 (1H, dd, J=2.4, 8.8 Hz), 6.12 (1H, s), 3.63 (2H, s), 3.39 (6H, s), 2.38 (3H, s), 1.02 (3H, t, J=7.0 Hz); FT-IR (KBr) cm^{-1}: 3244, 2929, 1658, 1653; ESI-MS m/z: 415.2 $(M+H)^+$. HR-MS: Calcd for $C_{22}H_{24}ClN_2O_4$ $(M+H)^+$: 415.1419, 417.1399. Found 415.1424, 417.1431.

***N*-3-Methoxypropyl-(1-*p*-chlorobenzoyl-5-hydroxy-2-methylindole)-3-acetamide (13)** Compound **13** was obtained in a similar manner to the synthesis of **3** from **11** using 3-methoxy propylamine. The crude product was purified by chromatography on silica gel with $CHCl_3$: acetone = 9 : 1 to give **13** (132 mg, 54.9%) as a pale yellow solid: mp 132—134 °C; ^{1}H-NMR ($CDCl_3$) δ: 7.73 (1H, s), 7.66 (2H, d, J=9.0 Hz), 7.47 (2H, d, J=7.6 Hz), 6.90 (1H, d, J=2.0 Hz), 6.84 (1H, d, J=8.8 Hz), 6.66 (1H, dd, J=2.4, 8.8 Hz), 6.46 (1H, t, J=5.2 Hz), 3.61 (2H, s), 3.33 (4H, m), 3.02 (3H, s), 2.36 (3H, s), 1.67 (2H, q, J=6.0 Hz); FT-IR (KBr) cm^{-1}: 3201, 2928, 1664, 1635; ESI-MS m/z: 415.2 $(M+H)^+$. HR-MS: Calcd for $C_{22}H_{24}ClN_2O_4$ $(M+H)^+$: 415.1419, 417.1399. Found 415.1384, 417.1408.

Inhibition of COX Activity Inhibition of COX activity was assayed by using the Colorimetric COX (ovine) Inhibitor Screening Assay kit (Cayman Chemical, No. 760111, lot; 194562, 040471, 0407481, 0408012, Michigan, U.S.A.). This assay measures the heme-catalyzed hydroperoxidase activity of ovine COX by monitoring the appearance of oxidized *N*,*N*,*N*′,*N*′-tetramethyl-*p*-phenylenediamine (TMPD).[26] Dimethylsulfoxide (DMSO) (10 μl, control) or a solution of the studied compound in DMSO (10^{-2}—10^{-8} M) was added to a 96-well plate with 0.1 M Tris–HCl assay buffer (pH 8.0) (150 μl), 4.4% solution of heme in DMSO (10 μl) and a solution of ovine COX-1 or COX-2 in 80 mM Tris–HCl (pH 8.0) containing 0.1% Tween 20 and 300 mM diethyldithiocarbamate. After 5 min of preincubation at room temperature, a solution of TMPD (20 μl) and arachidonic acid (20 μl) dissolved in 1.1 M ethanol containing 5 mM KOH was added to the mixture. The mixture was incubated for a further 5 min and the absorbance was measured on a plate reader at 595 nm. Celecoxib and indomethacin were used as the reference compounds. The results are shown in Table 1.

^{11}C-Labeling of Compounds 1, 2, 3, 5 and 6 [^{11}C]Methyl triflate was trapped in acetone (250 μl) containing each precursor (0.25 mg, 0.54—0.60 mmol) at room temperature. Immediately before starting the radiosynthesis, a solution of aqueous NaOH was added in the reaction vessel: 3 μl of 0.2 M NaOH (0.60 mmol, 1 eq) for **1** and 5 μl of 1 M NaOH (5 μmol) for the other four compounds. After trapping [^{11}C]methyl triflate, a mixture (1.4 ml) of H_2O and the mobile phase of HPLC (1 : 1) was added and then the reaction mixture was applied to a semi-preparative HPLC column (YMC-Pack ODS-A, 10 mm×150 mm, YMC, Kyoto, Japan). At a 5 ml/min flow rate, a mixture of acetonitrile (MeCN) and H_2O was used for the mobile phase: MeCN : H_2O = 9 : 1 for [^{11}C]**1** (retention time (t_R): 6.1 min for [^{11}C]**1** and 3.8 min for **7**) and [^{11}C]**2** (t_R: 5.6 min for [^{11}C]**2** and 3.9 min for **8**); 7 : 3 for

[^{11}C]**3** (t_R: 7.2 min for [^{11}C] **3** and 4.0 min for **9**); and 6 : 4 for [^{11}C]**5** (t_R: 6.5 min for [^{11}C] **5** and 3.6 min for **12**) and [^{11}C]**6** (t_R: 5.9 min for [^{11}C] **6** and 3.3 min for **13**). Each [^{11}C]product fraction was collected in a flask containing a solution of L-ascorbic acid (0.1 ml, 100 mg/ml) in water and evaporated to dryness. The residue was dissolved in physiological saline containing 0.125% Tween 80. The labeled compound was analyzed by HPLC: TSKgel Super-ODS column (4.6 mm×100 mm, Tosoh, Tokyo, Japan); mobile phase, MeCN : H_2O=8 : 2 for [^{11}C]**1** and [^{11}C]**2**; 7 : 3 for [^{11}C]**3**; and 6 : 4 for [^{11}C]**5** and [^{11}C]**6**; and 1.0 ml/min flow rate. Retention times were 3.6 min for [^{11}C]**1**, 3.0 min for [^{11}C]**2**, 5.3 min for [^{11}C]**3**, 3.0 min for [^{11}C]**5** and 2.7 min for [^{11}C]**6**. The results are shown in Table 2.

Octanol–Water Partition Coefficient A mixture of each radiotracer (1.5—2.8 MBq) in octanol (4 ml for [^{11}C]**1**, [^{11}C]**2**, [^{11}C]**5** and [^{11}C]**6**, or 2 ml for [^{11}C]**3**) and an equivalent volume of phosphate buffered saline (PBS; 1/15 M, pH 7.4) was vortexed at 20 s×3 times and then centrifuged (1500 rpm for 1 min). An aliquot was taken from the organic phase (0.2 ml) and the aqueous phase (0.2 ml for [^{11}C]**1** and [^{11}C]**2**, 0.4 ml for [^{11}C]**3**, 1 ml for [^{11}C]**5** and [^{11}C]**6)** and the ^{11}C radioactivity was measured in an auto-gamma-counter. The octanol–water partition coefficient was calculated as the radioactivity ratio between the octanol and aqueous phases, and its mean logarithm ($\log P_{7.4}$) was determined to express as lipophilicity. The results are shown in Table 2.

Tissue Distribution of Radiotracers in Mice Male ddY mice (8—9 weeks old, body weight; 34—41 g) were used for the following experiments: (A) tissue distribution, (B) a blocking study to determine specific uptake and (C) cyclosporine A (CysA) treatment, and all mice were injected with each radiotacer (2.0—2.8 MBq/8—97 pmol) in a physiological saline (0.2 ml) containing 0.125% Tween 80 through the tail vein.

Group A mice were killed by cervical dislocation 1, 5, 15, 30 and 60 min after radiotracer injection. Group B mice received the following blocker solution (1 mg/kg per animal, 0.1 ml), carrier compounds (**1**, **2**, **3**, **5**, or **6**), NS-398, celecoxib, and indomethacin dissolved in DMSO, co-injected with each radiotracer. In the control mice the same amount of DMSO was co-injected. The mice were killed at 30 min after injection for [^{11}C]**1**, [^{11}C]**2** and [^{11}C]**3** and at 15 min for [^{11}C]**5** and [^{11}C]**6**. Group C mice were treated with an intravenous injection of cyclosporine A (CysA, Sandimmun®, Tokyo, Japan) (50 mg/kg)[46,47] dissolved in a physiological saline 30 min prior to the tracer injection. Each radiotracer was intravenously injected into CysA-treated and control mice, and the radioactivity levels of the brain and blood were measured at 30 min for [^{11}C]**2** and [^{11}C]**3**, and at 15 min for [^{11}C]**5** and [^{11}C]**6**.

The ^{11}C in the samples obtained was counted with an auto-gamma-counter and the tissues were weighed. The tissue uptake of ^{11}C was expressed as a percentage of injected dose per gram of tissue (%ID/g). Student's unpaired *t*-test was used to compare the groups in the pharmacological experiments; a value of $p<0.05$ was considered statistically significant. The results are shown in Table 3, Table 5 and Table 6.

Metabolite Analysis Each tracer (20—100 MBq/230—1500 pmol) was intravenously injected into the mice (8—9 weeks old), and 30 min later they were killed by cervical dislocation (n=3). The blood was removed by heart puncture using a heparinized syringe and the brain was removed.

The blood was centrifuged at 7000×***g*** for 1 min at 4 °C to obtain the plasma, which (50 μl) was denatured with 0.5 ml of 10% trichloroacetic acid (TCA) in MeCN or a 1 : 1 mixture of MeCN and 50 mM CH_3COOH–CH_3COONa (50 : 50). The mixture was centrifuged under the same conditions, and the precipitate was re-suspended in 0.5 ml of the same solution, followed by centrifugation. This procedure was repeated twice. The combined supernatant was diluted with an equal portion of 50 mM CH_3COOH–CH_3COONa (50 : 50). No decomposition of the radiotracers under the conditions treated was confirmed.

The cerebral cortex (50 mg) was homogenized in 1.0 ml of ice-cold 10% TCA in MeCN or an ice-cold 1 : 1 mixture of MeCN and 50 mM CH_3COOH–CH_3COONa (50 : 50). The homogenate was then treated as described in the plasma sample.

After protein elimination, recovery of the radioactivity in the soluble fractions was 82—98% for the plasma samples and 73—95% for brain samples of each radiotracer.

The supernatant samples obtained from the plasma and brain homogenates were applied to HPLC analysis using a 10-μm Radial-Pak C_{18} column and a 6-μm Prep Nova-pak 60A equipped with an RCM 8×10 module (8 mm×100 mm, Waters, Millford, MA, U.S.A.) for [^{11}C]**1** and [^{11}C]**3** and for [^{11}C]**1** and [^{11}C]**2**, respectively, and a reversed phase column (YMC-Pack ODS-A, 10 mm×250 mm, YMC, Kyoto, Japan). The mobile phase consisted of a 8 : 2 mixture of MeCN and a 50 mM CH_3COOH–CH_3COONa buffer (50 : 50) for [^{11}C]**1** and [^{11}C]**2**, and a 7 : 2 mixture of the same solvent for [^{11}C]**3**, [^{11}C]**5** and [^{11}C]**6** at a flow rate of 2—3 ml/min. The results are shown in Table 4.

Acknowledgments The financial support of the program for the Creation of Innovation Centers for Advanced Interdisciplinary Research Areas from Special Coordination Funds for Promoting Science and Technology (SCF) commissioned by the Ministry of Education, Culture, Sports, Science and Technology (MEXT) of Japan is gratefully acknowledged. We appreciate for the technical supports from the Research Support Center, Graduate School of Medical Sciences, Kyushu University, and Mr. Kunpei Hayashi for radiosynthesis.

References

1) Crofford L. J., *J. Rheumatol.*, **49**, 15—19 (1997).
2) Fitzpatrick F. A., *Curr. Pharm. Des.*, **10**, 577—588 (2004).
3) Blobaum A. L., Marnett L. J., *J. Med. Chem.*, **50**, 1425—1441 (2007).
4) Chandrasekharan N. V., Dai H., Roos K. L., Evanson N. K., Tomsik J., Elton T. S., Simmons D. L., *Proc. Natl. Acad. Sci. U.S.A.*, **99**, 13926—13931 (2002).
5) Mitchell J. A., Warner T. D., *Br. J. Pharmacol.*, **128**, 1121—1132 (1999).
6) Hewett S. J., Bell S. C., Hewett J. A., *Pharmacol. Ther.*, **112**, 335—357 (2006).
7) Minghetti L., *J. Neuropathol. Exp. Neurol.*, **63**, 901—910 (2004).
8) Lleo A., Galea E., Sastre M., *Cell. Mol. Life Sci.*, **64**, 1403—1418 (2007).
9) FizGerald G.A., *Nat. Rev. Drug Discov.*, **2**, 879—890 (2003).
10) de Vries E. F. J., *Curr. Pharm. Des.*, **12**, 3847—3856 (2006).
11) Fujisaki Y., Kawamura K., Wang W.-F., Ishiwata K., Yamamoto F., Kuwano T., Ono M., Maeda M., *Ann. Nucl. Med.*, **19**, 617—625 (2005).
12) Tanaka M., Fujisaki Y., Kawamura K., Ishiwata K., Qinggeletu, Yamamoto F., Mukai T., Maeda M., *Biol. Pharm. Bull.*, **29**, 2087—2094 (2006).
13) McCarthy T. J., Sheriff A. U., Graneto M. J., Talley J. J., Welch M. J., *J. Nucl. Med.*, **43**, 117—124 (2002).
14) de Vries E. F. J., van Waarde A., Buursma A. R., Vaalburg W., *J. Nucl. Med.*, **44**, 1700—1706 (2003).
15) Toyokuni T., Kumar J. S. D., Walsh J. C., Shapiro A., Talley J. J., Phelps M. E., Herschman H. R., Barrio J. R., Satyamurthy N., *Bioorg. Med. Chem. Lett.*, **15**, 4699—4702 (2005).
16) Prabhakaran J., Underwood M. D., Parsey R. V., Arango V., Majo V. J., Simpson N. R., Van Heertum R., Mann J. J., Kumar J. S. D., *Bioorg. Med. Chem.*, **15**, 1802—1807 (2007).
17) Wuest F., Kniess T., Bergmann R., Pietzsch J., *Bioorg. Med. Chem.*, **16**, 7662—7670 (2008).
18) de Vries E. F. J., Doorduin J., Dierckx R. A., van Waarde A., *Nucl. Med. Biol.*, **35**, 35—42 (2008).
19) Singh P., Mittal A., *Mini Rev. Med. Chem.*, **8**, 73—90 (2008).
20) Clark D. E., *Drug Discov. Today*, **8**, 927—933 (2003).
21) Kalgutkar A. S., Marnett A. B., Crews B. C., Remmel R. P., Marnett L. J., *J. Med. Chem.*, **43**, 2860—2870 (2000).
22) Kalgutkar A. S., Crews B. C., Saleh S., Prudhomme D., Marnett L. J., *Bioorg. Med. Chem.*, **13**, 6810—6822 (2005).
23) Kalgutkar A. S., Crews B. C., Rowlinson S. W., Marnett A. B., Kozak K. R., Remmel R. P., Marnett L. J., *Proc. Natl. Acad. Sci. U.S.A.*, **97**, 925—930 (2000).
24) Uddin Md. J., Crews B. C., Blobaum A. L., Kingsley P. J., Ghebreselasie K., Saleh S. S., Clanton J. A., Baldwin R. M., Marnett L. J., *J. Labelled Compd. Radiopharm.*, **52**, 387—393 (2009).
25) Uddin Md. J., Crews B. C., Blobaum A. L., Kingsley P. J., Gorden D. L., Mclntyre J. O., Matrisian L. M., Subbaramaiah K., Dannenberg A. J., Piston D. W., Marnett L. J., *Cancer Res.*, **70**, 3618—3627 (2010).
26) Sharma R., Sainy J., Chaturvedi S. C., *Acta Pharm.*, **58**, 317—326 (2008).
27) Wilson A. A., Jin L., Garcia A., DaSilva J. N., Houle S., *Appl. Radiat. Isot.*, **54**, 203—208 (2001).
28) Dischino D. D., Welch M. J., Kilbourn M. R., Raichle M. E., *J. Nucl. Med.*, **24**, 1030—1038 (1983).
29) Waterhouse R. N., *Mol. Imaging Biol.*, **5**, 376—389 (2003).
30) Boyer D., Bauman J. N., Walker D. P., Kapinos B., Karki K., Kalgutkar A. S., *Drug Metab. Dispos.*, **37**, 999—1008 (2009).
31) Davis N. M., Skjodt N. M., *Clin. Pharmacokinet.*, **38**, 377—392 (2000).

32) Parepally J. M. R., Mandula H., Smith Q. R., *Pharm. Res.*, **23**, 873—881 (2006).
33) Rapoport S. I., Arai T., Wakabayashi S., Channing M. A., Dunn B. B., Der M. G., Bell J. M., Herscovitch P., Eckelman W. C., Chang M. C., *J. Nucl. Med.*, **36**, 2261—2267 (1995).
34) Chang M. C., Arai T., Freed L. M., Wakabayashi S., Channing M. A., Dunn B. B., Der M. G., Bell J. M., Sasaki T., Herscovitch P., Eckelman W. C., Rapoport S. I., *Brain Res.*, **755**, 74—83 (1997).
35) Giovacchini G., Chang M. C., Channing M. A., Toczek M., Mason A., Bokde A. L., Connolly C., Vuong B.-K., Ma Y., Der M. G., Doudet D. J., Herscovitch P., Eckelman W. C., Rapoport S. I., Carson R. E., *J. Cereb. Blood Flow Metab.*, **22**, 1453—1462 (2002).
36) Habgood M. D., Begley D. J., Abbott N. J., *Cell. Mol. Neurobiol.*, **20**, 231—253 (2000).
37) Remmel R. P., Crews B. C., Kozak K. R., Kalgutkar A. S., Marnett L. J., *Drug Metab. Dispos.*, **32**, 113—122 (2004).
38) Cecchell R., Berezowski V., Lundquist S., Culot M., Renftel M., Dehouck M. P., Fenart L., *Nat. Rev. Drug Discov.*, **6**, 650—661 (2007).
39) Elsinga P. H., Hendrikse N. H., Bart J., Vaalburg W., van Waarde A., *Curr. Pharm. Des.*, **10**, 1493—1503 (2004).
40) Ishiwata K., Kawamura K., Yanai K., Hendrikse N. H., *J. Nucl. Med.*, **48**, 81—87 (2007).
41) Zrieki A., Farinotti R., Buyse M., *Pharm. Res.*, **25**, 1991—2001 (2008).
42) Niwa T., Yamamoto S., Saito M., Shiraga T., Takagi A., *Yakugaku Zasshi*, **127**, 209—216 (2007).
43) Wacher V. J., Silverman J. A., Zhang Y., Benet L. Z., *J. Pharm. Sci.*, **87**, 1322—1330 (1998).
44) Kajosaari L. I., Niemi M., Neuvonen M., Laitila J., Neuvonen P. J., Backman J. T., *Clin. Pharmacol. Ther.*, **78**, 388—399 (2005).
45) Penning T. D., Talley J. J., Bertenshaw S. R., Carter J. S., Collins P. W., Docter S., Graneto M. J., Lee L. F., Malecha J. W., Miyashiro J. M., Rogers R. S., Rogier D. J., Yu S. S., Anderson G. D., Burton E. G., Cogburn J. N., Gregory S. A., Koboldt C. M., Perkins W. E., Seibert K., Veenhuizen A. W., Zhang Y. Y., Isakson P. C., *J. Med. Chem.*, **40**, 1347—1365 (1997).
46) de Vries E. F. J., Kortekaas R., van Waarde A., Dijkstra D., Elsinga P. H., Vaalburg W., *J. Nucl. Med.*, **46**, 1384—1392 (2005).
47) Evens N., Bosier B., Lavey B. J., Kozlowski J. A., Vermaelen P., Baudemprez L., Busson R., Lambert D. M., Van Laere K., Verbruggen A. M., Bormans G. M., *Nucl. Med. Biol.*, **35**, 793—800 (2008).